

On minimal realization of Topological Lorentz Structures with one-loop Seesaw extensions in A_4 Modular Symmetry

Monal Kashav*and Surender Verma†

*Department of Physics and Astronomical Science,
Central University of Himachal Pradesh, Dharamshala 176215, INDIA.*

Abstract

The topological classification of one-loop Weinberg operator at dimension-5 leads to systematic categorization of one-loop neutrino mass models. All one-loop neutrino mass models must fall in one of these categories. Among these topological categories, loop extension of canonical seesaw scenarios is interesting in light of the current LHC run. Apart from one-loop contribution, these extensions result in dominant tree-level contribution to neutrino masses. The immediate remedy to obtain dominant one-loop contribution requires combination of flavor symmetries and enlarged field content. Alternatively, in this work, we propose a minimal way of realizing the topological structures with dominant one-loop contribution using modular variant of the permutation symmetries. In such a realization, no new fields are needed apart from those permitted by the topology itself. For the first time, we have realized one such topological Lorentz structure(T4-2- i) pertaining to one-loop extension of Type-II seesaw using modular A_4 symmetry. Here, modular weights play an important role in suppressing tree-level terms and stabilizing the particles running in the loop(N_i , ρ and ϕ), thus, making them suitable dark matter candidates. In this work, we have explored the possibility of fermionic dark matter candidate where right-handed neutrino (N_1) is assumed to be lightest. We have, also, analyzed the compatibility of the model with neutrino oscillation data and obtained model predictions for effective Majorana mass M_{ee} and CP violation. Furthermore, the predictions on relic density of dark matter and its direct detection considering bound on lepton flavor violating process, $\mu \rightarrow e\gamma$ have, also, been investigated.

1 Introduction

The Weinberg operator at the lowest dimension, $d = 5$, allows lepton number violation by two units ($\Delta L = 2$) and explains the smallness of neutrino masses [1]. UV completion of the Weinberg operator leads to well-known Type-I [2,3], Type-II [4–6] and Type-III [7] seesaw paradigms. In conventional Type I/II/III seesaw mechanisms, new heavy degree of freedom suppresses the neutrino mass. These heavy degrees of freedom are not accessible at current Large Hadron Collider (LHC) runs. Apart from the introduction of new degrees of freedom, fine-tuning of Yukawa couplings is required to correctly explain the small neutrino masses. Besides these seesaw scenarios, a more promising framework is radiative generation of neutrino mass at one-loop level as it explains non-zero neutrino mass and dark matter, simultaneously. Furthermore, some of LHC accessible new physics variants for neutrino mass generation are inverse [8] or linear seesaw [9,10] mechanisms at tree level, radiative mass generation through loop integrals [11], SUSY models with R-parity violation [12–14] to name a few.

In general, Weinberg operator at one-loop [15] and two-loop [16] leads to systematic topological classification of neutrino mass models. In fact, Weinberg operator leads to six topologies T_i ($i=1,2,\dots,6$) of one-loop diagrams with four external legs [15]. Out of these six topologies T_2 is discarded on the basis of dimensional

*Electronic address: monalkashav@gmail.com

†Electronic address: s_7verma@hpcu.ac.in

disagreements. The topologies T3, T5 and T6 have one Lorentz structure whereas T1, T4 can have different topological structures depending on whether the fields running in the loop are of scalar or fermionic nature,

$$\begin{aligned} \text{T1:} & \quad \text{T1-}i; \text{T1-}ii; \text{T1-}iii, \\ \text{T4:} & \quad \text{T4-1-}i; \text{T4-1-}ii; \text{T4-2-}i; \text{T4-2-}ii; \text{T4-3-}i; \text{T4-3-}ii. \end{aligned}$$

All the Lorentz structures corresponding to these six topologies can be grouped in three categories *viz.*, (i) divergent one-loop extensions of seesaw: T4-1-*i*, T4-2-*ii*, T4-3-*ii*, T5, T6 (ii) finite one-loop diagrams giving leading contribution to non-zero neutrino mass naturally: T1-*i*, T1-*ii*, T1-*iii*, T3 and (iii) finite one-loop extension of seesaw: T4-1-*ii*, T4-2-*i*, T4-3-*i*. For the topological Lorentz structures of T1 and T3 (category (ii)), it is always possible to have one-loop dominant contribution to non-zero neutrino mass by forbidding the tree-level contribution using discrete or U(1) symmetry [15]. Further, on the basis of symmetry arguments it can be shown (discussed in Section 3.1) that T4 topology (category (iii)) carries dominant tree-level contribution in addition to one-loop diagram contribution regardless of imposition of discrete or U(1) symmetry. In category (iii), the topological Lorentz structures T4-1-*ii* and T4-2-*i* are one-loop extensions of Type-II seesaw whereas T4-3-*i* corresponds to one-loop extension of Type-I/III seesaw scenario.

The divergent topological diagrams (category (i)) require counter-terms to absorb the divergences which are in turn its tree-level realizations. The topological Lorentz structures of category (ii) such as T1-*i* have been realized in Refs. [17–19] while the well-studied Zee model [20] is a realization of T1-*ii* Lorentz structure. Also, implications of Lorentz structures T1-*iii* and T3 have been discussed in Ref. [21]. In category (iii), the tree-level contribution to neutrino masses dominates. In Ref. [22], the authors have discussed the possible realization of T4-1-*ii* topological structure wherein the tree-level terms were inhibited using discrete symmetry and the neutrino masses were generated by dimension, $d = 7$ operator. One of $U(1)_{B-L}$ model proposed in Ref. [23] reduces to topology T4-3-*i* with one-loop dominant contribution to neutrino masses. In Ref. [15], it was suggested that for category (iii) topological Lorentz structures implementation of Z_2 symmetry and assuming fermion running in the loop to be of Majorana nature leads to one-loop dominant contribution to neutrino masses, provided all couplings conserves the lepton number. In this way one can forbids the tree-level terms effectively leading to dominant one-loop seesaw contributions. However, neutrino mass generation, in general, leads to lepton number violation in realistic models. It is difficult to realize T4-2-*i* with dominant one-loop contribution since scalar triplet couples to lepton doublets leading to tree-level dominant contribution. In the existing literature, one such attempt has been made employing D_4 , cyclic symmetries with enlarged field content wherein lepton number is violated by right-handed Majorana neutrino mass couplings [24]. Here, we argue that one may not require additional fields (fields other than required by the topology) to suppress the tree-level contribution if we work within the paradigm of modular symmetry. As an example, we have constructed a possible realization of T4-2-*i* topology based on A_4 modular symmetry.

In this work, we propose a realization of one-loop topology T4-2-*i* which, essentially, requires two scalar doublets (ϕ, ρ), one scalar triplet (Δ) and fermionic field(s) ψ . Keeping in view the advantage of modular symmetries over discrete symmetries that Yukawa couplings transform like other scalar or fermionic fields, we realize the topology using the A_4 modular symmetry in a minimal way. The field content of the model includes fields permitted by the topology only which is more economical and minimalist than the model proposed in Ref. [24]. The lepton number violation is manifested by assuming fermions running inside the loop as right-handed Majorana neutrinos. The tree-level Dirac neutrino mass term (emanating from the coupling of Higgs field with lepton doublet and right-handed Majorana neutrino) and tree-level contribution from scalar triplet is inhibited, successfully, by assigning suitable weights under the A_4 modular symmetry. Consequently, neutrino masses are generated by one-loop Type-II seesaw without the use of additional beyond standard model (BSM) field(s). The dark matter candidate(s) running in the loop are stabilized by assigning odd modular weights under A_4 modular group. We analyse the viability of the model under current neutrino oscillation data. Also, considering the possibility of fermionic dark matter, we have obtained the prediction on relic density of dark matter consistent with upper bound on branching ratio of lepton flavor violating (LFV) process $\mu \rightarrow e\gamma$. Furthermore, the implications of the model for direct detection of dark matter are obtained.

The paper is organized as follows. Section 2 is devoted for the possible realization of T4-2-*i* topological Lorentz structure. In this section, we first reproduce some general features of T4-2-*i* topology to make

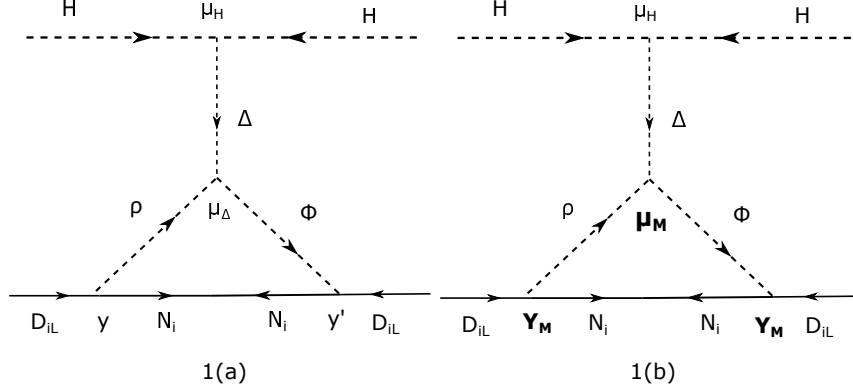


Figure 1: General T4-2-i topological structure (Fig. 1(a)) wherein Yukawa couplings are constants and effect of A_4 modular symmetry to inhibit the tree-level contribution (Fig. 1(b)). The couplings μ_{H_M} , μ_{Δ_M} , Y_M and Y'_M in Fig. 1(b) transform under the A_4 modular symmetry.

context of the problem and then propose possible scenario for the suppression of tree-level couplings based on A_4 modular symmetry. Further, we have illustrated possible realization of the model in supersymmetric (SUSY) framework. The numerical analysis based on the discussions presented in Section 2, has been carried out in Section 3. In Section 4, we discuss the framework of calculation for relic density, spin independent cross-section for direct detection of dark matter and lepton flavor violation. Finally, we brief the conclusions in Section 5. The preliminaries about the modular symmetry and its connection to the permutation groups are discussed in Appendix A.

2 $\Gamma_3 \simeq A_4$ based T4-2-i Model

In this section, firstly we discuss the general features of T4-2-i topology to make relevant context of the problem. Also, using symmetry arguments it is shown that in topology T4 tree-level terms are always invariant and dominating regardless of imposition of discrete or U(1) symmetry. Secondly, we propose a realization of this topology by assigning suitable charge assignments to the field content and Yukawa couplings under A_4 modular invariance (see Appendix A for details).

2.1 General features of T4-2-i Topology

In general, finite diagrams of T4 topology are one-loop extensions of canonical Type-I/II/III seesaw scenarios. Particularly, T4-2-i topological Lorentz structure is one-loop extension of Type-II seesaw. It extends the SM with two scalar doublets (ρ, ϕ) and heavy Majorana right-handed neutrinos (N_i) as shown in Fig. 1(a). It is to be noted that

1. If scalar doublet acquires the vev , one-loop diagram reduces to tree-level diagram of canonical Type-II seesaw.
2. The tree-level contribution act as leading contribution in addition to one-loop contribution to neutrino masses.

It is straightforward to understand it from Fig. 1(a): In order to have topology T4-2-i at one-loop level, all the vertices should be allowed by invariance under the new symmetry. Let Q_j be the quantum number under the new symmetry. For the vertex $\mu_H H \Delta^\dagger H$ to be allowed, we require $2Q_H + Q_\Delta = 0$. Also, invariance of vertices $\mu_\Delta \Delta \rho \phi^\dagger$, Yukawa couplings y and y' require

$$Q_\Delta - Q_\rho + Q_\phi = 0,$$

Symmetry	\bar{D}_{eL}	$\bar{D}_{\mu L}$	$\bar{D}_{\tau L}$	e_R	μ_R	τ_R	N_1	N_2	N_3	H	Δ	$\tilde{\phi}$	ρ
$SU(2)_L$	2	2	2	1	1	1	1	1	1	2	3	2	2
$U(1)_Y$	1	1	1	-2	-2	-2	0	0	0	1	2	-1	-1
A_4	1	1''	1'	1	1'	1''	1	1'	1''	1	1	1	1
$-k_I$	2	2	2	-2	-2	-2	-3	-3	-3	0	0	-3	-3

Table 1: The field content of the model and respective charge assignments under $SU(2)_L$, $U(1)_Y$, A_4 , including modular weights.

Y_m^n	Y_1^4	$Y_{1'}^4$	Y_1^6	Y_1^8	$Y_{1'}^8$	$Y_{1''}^8$	Y_1^{10}	$Y_{1'}^{10}$
A_4	1	1'	1	1	1'	1''	1	1'
$-k_I$	4	4	6	8	8	8	10	10

Table 2: The transformations of higher order Yukawa couplings under A_4 modular symmetry.

$$Q_{D_L} + Q_{N_i} - Q_\rho = 0,$$

$$Q_{D_L} - Q_{N_i} + Q_\phi = 0,$$

respectively, which, further reduces to $2Q_{D_L} + Q_\Delta = 0$ implying that tree-level Type-II seesaw term is always present. It is evident from above analysis that if vertex $\mu_H H \Delta^\dagger H$ is allowed, tree-level term is also allowed. However, in order to have dominant one-loop contribution the tree-level term must be inhibited while the vertex $\mu_H H \Delta^\dagger H$ should be allowed under the new symmetry invariance. Similar problem arises in other finite diagrams of T4 topological Lorentz structures.

2.2 Implications of A_4 Modular Symmetry

A_4 Modular symmetry have even modular weights for Yukawa couplings which are treated as constant in conventional flavor symmetric models. The matter fields can have integral modular weights such that sum of modular weights vanishes for an invariant term of Lagrangian (as discussed in Appendix A).

In order to realize the topology T4-2- i with dominant one-loop contribution, we need to ensure following:

1. There is no tree-level contribution from scalar triplet i.e. $2Q_L + Q_\Delta \neq 0$ while the vertex $\mu_H H \Delta^\dagger H$ should be allowed.
2. The Dirac neutrino mass term emanating from the coupling of Higgs field with lepton doublet and right-handed Majorana neutrino is inhibited.
3. Essentially, the vertices with couplings μ_Δ , y and y' (Fig. 1(a)) should be allowed such that neutrino mass generation is manifested at one-loop level via scalar triplet only.

Under A_4 modular paradigm, we employ fields permitted by the topology only i.e. two scalar doublets (ϕ , ρ), one scalar triplet (Δ) and assuming the fermions inside the loop as right-handed Majorana neutrinos. The field content of the model and corresponding modular weights are given in Table 1. Also, the transformations of Yukawa couplings under A_4 modular symmetry are shown in Table 2.

Scalar potential terms: Firstly, we assume Higgs field (H) and scalar triplet (Δ) as trivial A_4 singlets with zero weight so that vertex $\mu_{H_M} H \Delta^\dagger H$ is allowed under A_4 modular symmetry. Secondly, the fields running inside the loop i.e. N_i , ρ and ϕ are assigned singlet representation under A_4 . Further, they have odd modular weights to ensure stability making them suitable dark matter candidates in the model (Table 1)). The above assignments requires μ_Δ mass coupling to have modular weight 6 so that the vertex $\mu_{\Delta_M} \Delta \phi^\dagger \rho$ is allowed.

Inhibition of tree-level terms: With the above charge assignments, the right-handed Majorana neutrino mass terms are allowed if Yukawa couplings transform as singlet of modular weight 6. Also, the charged lepton fields transform under A_4 modular symmetry such that charged lepton mass matrix is diagonal with modular weight 6. Consequent to the above discussion:

1. The Yukawa couplings y and y' have modular weight -4 which can be made invariant if Y_M and Y'_M acquire modular weight +4 i.e. $Y_1^4, Y_{1'}^4$, as shown in Fig. 1(b).
2. The tree-level Dirac term is not allowed since sum of modular weights is odd.
3. Also, the tree-level Type-II seesaw term is disallowed as sum of modular weight is positive and even.

Hence, tree-level contribution is suppressed due to the imposition of A_4 modular invariance, thus, resulting in dominant one-loop contribution to neutrino mass.

One-loop contribution to neutrino mass: The Yukawa Lagrangian for charged leptons under A_4 modular invariance is given by

$$\mathcal{L}_I = \alpha_l(\bar{D}_{eL}H e_R) + \beta_l(\bar{D}_{\mu L}H \mu_R) + \gamma_l(\bar{D}_{\tau L}H \tau_R), \quad (1)$$

where α_l, β_l and γ_l are coupling constants. After the spontaneous symmetry breaking, the Higgs field acquires the vacuum expectation value (vev), v_H . The resulting charged lepton mass matrix, M_l , is given by

$$M_l = \frac{v_H}{\sqrt{2}} \begin{pmatrix} \alpha_l & 0 & 0 \\ 0 & \beta_l & 0 \\ 0 & 0 & \gamma_l \end{pmatrix}. \quad (2)$$

With modular transformations given in Table 1 and 2, the Yukawa Lagrangian describing the neutrino mass generation at one-loop is given by

$$\begin{aligned} \mathcal{L}_{II} &= g_1(\bar{D}_{eL}\rho N_1 Y_1^4) + g_2(\bar{D}_{\mu L}\rho N_2 Y_1^4) + g_3(\bar{D}_{\tau L}\rho N_3 Y_1^4) \\ &+ k_1(\bar{D}_{eL}\rho N_3 Y_{1'}^4) + k_2(\bar{D}_{\mu L}\rho N_1 Y_{1'}^4) + k_3(\bar{D}_{\tau L}\rho N_2 Y_{1'}^4) \\ &+ a_1(\bar{D}_{eL}\tilde{\phi} N_1 Y_1^4) + a_2(\bar{D}_{\mu L}\tilde{\phi} N_2 Y_1^4) + a_3(\bar{D}_{\tau L}\tilde{\phi} N_3 Y_1^4) \\ &+ b_1(\bar{D}_{eL}\tilde{\phi} N_3 Y_{1'}^4) + b_2(\bar{D}_{\mu L}\tilde{\phi} N_1 Y_{1'}^4) + b_3(\bar{D}_{\tau L}\tilde{\phi} N_2 Y_{1'}^4) \\ &+ M'_1 \bar{N}_1^c N_1 Y_1^6 + M'_2 (\bar{N}_2^c N_3 Y_1^6 + \bar{N}_3^c N_2 Y_1^6), \end{aligned} \quad (3)$$

where g_i, k_i, a_i and b_i ($i = 1, 2, 3$) are coupling constants. Here, modular weights play the role of Z_2 symmetry stabilizing the dark matter candidates and inhibiting tree-level Yukawa couplings. The odd modular weights act as Z_2 odd charges which stabilizes the fields dictated by topology itself i.e. scalar doublets (ϕ, ρ) and right-handed Majorana neutrinos (N_1, N_2, N_3) running in the loop. The scalar doublets (ϕ, ρ) are inert having no vacuum expectation value (vev). The Lagrangian in Eqn. (3) results in the following Dirac Yukawa matrices,

$$y_\rho = \begin{pmatrix} g_1 Y_1^4 & 0 & k_1 Y_{1'}^4 \\ k_2 Y_{1'}^4 & g_2 Y_1^4 & 0 \\ 0 & k_3 Y_{1'}^4 & g_3 Y_1^4 \end{pmatrix}, \quad y_\phi = \begin{pmatrix} a_1 Y_1^4 & 0 & b_1 Y_{1'}^4 \\ b_2 Y_{1'}^4 & a_2 Y_1^4 & 0 \\ 0 & b_3 Y_{1'}^4 & a_3 Y_1^4 \end{pmatrix}. \quad (4)$$

Also, the right-handed Majorana neutrino mass matrix M_R is given by

$$M_R = \begin{pmatrix} M'_1 Y_1^6 & 0 & 0 \\ 0 & 0 & M'_2 Y_1^6 \\ 0 & M'_2 Y_1^6 & 0 \end{pmatrix}, \quad (5)$$

where M'_k ($k = 1, 2$) are right-handed neutrino mass scales of the bare mass terms. The right-handed neutrino masses M_k ($k = 1, 2, 3$) can be obtained by diagonalizing M_R using the unitary mixing matrix U_R i.e. $diag(M_1, M_2, M_3) = U_R M_R U_R^T$. In M_R -diagonal basis, the Dirac Yukawa matrices (Eqn. (4)) are given by

$$Y_\rho = y_\rho U_R; \quad Y_\phi = y_\phi U_R. \quad (6)$$

Using the Eqns. (4-6), the dominant one-loop contribution to neutrino mass is given by [15]

$$M_\nu = - \sum_k \frac{\mu_{\Delta_M} v^2}{m_\Delta^2} \mu_{H_M} [Y_\rho(M_k) Y_\phi^T] \mathcal{I}(M_\rho^2, M_\phi^2, M_k^2), \quad (7)$$

where μ_{Δ_M} and μ_{H_M} are couplings at vertices $\mu_{H_M} H \Delta^\dagger H$ and $\mu_{\Delta_M} \Delta \phi^\dagger \rho$ (Fig. 1(b)), respectively. The loop factor in the Eqn. (7) is given by

$$\begin{aligned} \mathcal{I}(M_\rho^2, M_\phi^2, M_k^2) = & - \left(\frac{1}{4\pi} \frac{M_\rho^2}{(M_\rho^2 - M_\phi^2)(M_\rho^2 - M_k^2)} \ln \frac{M_k^2}{M_\rho^2} \right. \\ & \left. + \frac{M_\phi^2}{(M_\phi^2 - M_\rho^2)(M_\phi^2 - M_k^2)} \ln \frac{M_k^2}{M_\phi^2} \right). \end{aligned} \quad (8)$$

The neutrino mass matrix emanating from Eqn. (7) is, in general complex and asymmetric. In order to have complex symmetric M_ν , the coupling constants must satisfy $g_i = a_i$ and $k_i = b_i$ ($i = 1, 2, 3$) equalities. It is to be noted that we have not considered the non-trivial relations amongst Yukawa couplings (as discussed in Ref. [24]) because, here, they transform under the A_4 modular symmetry. Also, it is to be noted that, the modular weight of loop particles *viz.* right-handed Majorana neutrinos (N_i), inert doublets (ρ, ϕ) is odd and thus, are suitable candidate for dark matter. Here, we have considered one such possibility, fermionic dark matter, by assuming mass of right-handed neutrino (M_1) to be smallest.

Thus, the neutrino mass matrix, M_ν , is proportional to $Y_\rho Y_\phi^T$ such that

$$M_\nu = \mathcal{K}(Y_\rho Y_\phi^T) \equiv \mathcal{K} \tilde{M}_\nu, \quad (9)$$

where $\mathcal{K} = M_1 \mathcal{I}(M_\rho^2, M_\phi^2, M_1^2)$ is the overall scale factor. The neutrino masses are given by $m_i = \mathcal{K} \tilde{m}_i$ ($i = 1, 2, 3$), where \tilde{m}_i are mass eigenvalues of $Y_\rho Y_\phi^T$. For Normal hierarchy, the scale factor is obtained using the atmospheric mass-squared difference Δm_{31}^2 (Table 5) as

$$\mathcal{K}^2 = \frac{\Delta m_{31}^2}{(\tilde{m}_3^2 - \tilde{m}_1^2)}. \quad (10)$$

Consequently, the solar mass-squared difference, in terms of \mathcal{K} , can be written as

$$\Delta m_{21}^2 = \mathcal{K}^2 (\tilde{m}_2^2 - \tilde{m}_1^2). \quad (11)$$

The neutrino mixing matrix U is obtained by diagonalizing M_ν using the transformation $U^T M_\nu U = \text{diag}(m_1, m_2, m_3)$. Since charged lepton mass matrix M_l (Eqn. (2)) is diagonal, the lepton mixing matrix is equal to neutrino mixing matrix i.e. $U_{PMNS} = U$, where U_{PMNS} is Pontecorvo–Maki–Nakagawa–Sakata matrix. The mixing angles can be evaluated using elements of the neutrino mixing matrix, U , as

$$\sin^2 \theta_{13} = |U_{13}|^2, \quad \sin^2 \theta_{12} = \frac{|U_{12}|^2}{1 - |U_{13}|^2}, \quad \sin^2 \theta_{23} = \frac{|U_{23}|^2}{1 - |U_{13}|^2}. \quad (12)$$

The Jarlskog rephasing CP invariant [25, 26] is given by

$$J_{CP} = \text{Im} [U_{11} U_{22} U_{12}^* U_{21}^*], \quad (13)$$

while other two CP invariants I_1 and I_2 related to Majorana phases (α, β) are

$$I_1 = \text{Im} [U_{11}^* U_{12}], \quad I_2 = \text{Im} [U_{11}^* U_{13}]. \quad (14)$$

Another important parameter to investigate is the effective Majorana neutrino mass (M_{ee}) which can shed light on the nature of neutrino being Dirac or Majorana particle. The effective Majorana mass is given by

$$M_{ee} = \left| \sum_{i=1}^3 U_{1i} m_i \right|. \quad (15)$$

The viability of model with neutrino oscillation data (Table 5) and its predictions for M_{ee} and CP violation is discussed in the next section.

Symmetry	\hat{D}_{eL}	$\hat{D}_{\mu L}$	$\hat{D}_{\tau L}$	e_R^c	μ_R^c	τ_R	N_1^c	N_2^c	N_3^c
$SU(2)_L$	2	2	2	1	1	1	1	1	1
$U(1)_Y$	-1	-1	-1	-2	-2	-2	0	0	0
A_4	1	1''	1'	1	1'	1''	1	1'	1''
$-k_I$	2	2	2	-2	-2	-2	-3	-3	-3

Table 3: The superfield content of the model and respective charge assignments under $SU(2)_L$, $U(1)_Y$, A_4 including modular weights.

Symmetry	H_u	H_d	ϕ_u	ϕ_d	ρ_u	ρ_d	Δ_u	Δ_d
$SU(2)_L$	2	2	2	2	2	2	3	3
$U(1)_Y$	1	-1	1	-1	1	-1	-2	2
A_4	1	1	1	1	1	1	1	1
$-k_I$	0	0	-3	-3	-3	-3	0	0

Table 4: The superfield content of the scalar sector of the model and respective charge assignments under $SU(2)_L$, $U(1)_Y$, A_4 including modular weights.

2.3 Supersymmetric (SUSY) realization of the Model

The superfield in the θ -expansion is given by [27]

$$\Phi = \phi_m + \sqrt{2}\theta.\psi_m + \theta^2 F_m, \quad (16)$$

where, ϕ_m is the scalar field, θ is the Grassmann variable, ψ_m is spinor field and F_m is auxiliary field. Since, SUSY transformation commutes with gauge transformation, superfields have same quantum numbers under the SM gauge group as shown in Table 3. The superfields \hat{D}_{iL} are defined as left chiral superfield lepton doublet, i_R^c are right-handed CP -conjugated charged lepton superfields where $i = e, \mu, \tau$. The CP -conjugated right-handed neutrino fields are defined as N_j^c where $j = 1, 2, 3$. The SUSY invariant interactions of superfields are obtained from the holomorphic terms (F-terms) of the superpotential which do not contain the H^\dagger terms leading to massless fermions. The second Higgs field $H_d = (H_d^0, H_d^-)$ play the role of H^\dagger while $H_u = (H_u^+, H_u^0)$ is the usual SM Higgs field. Here, d, u represent corresponding field giving mass to down-type and up-type quarks. Therefore, scalar sector has twice the number of fields in SM as shown in Table 4. The superpotential responsible for the masses of charged lepton is given by

$$\mathcal{W}_I = \alpha_l(\hat{D}_{eL}H_d e_R^c) + \beta_l(\hat{D}_{\mu L}H_d \mu_R^c) + \gamma_l(\hat{D}_{\tau L}H_d \tau_R^c), \quad (17)$$

where α_l , β_l and γ_l are coupling constants. Also, the superpotential responsible for neutrino mass generation is given by

$$\begin{aligned} \mathcal{W}_{II} &= g_1(\hat{D}_{eL}\rho_d N_1^c Y_1^4) + g_2(\hat{D}_{\mu L}\rho_d N_2^c Y_1^4) + g_3(\hat{D}_{\tau L}\rho_d N_3^c Y_1^4) \\ &+ k_1(\hat{D}_{eL}\rho_d N_3^c Y_1^4) + k_2(\hat{D}_{\mu L}\rho_d N_1^c Y_1^4) + k_3(\hat{D}_{\tau L}\rho_d N_2^c Y_1^4) \\ &+ a_1(\hat{D}_{eL}\phi_d N_1^c Y_1^4) + a_2(\hat{D}_{\mu L}\phi_d N_2^c Y_1^4) + a_3(\hat{D}_{\tau L}\phi_d N_3^c Y_1^4) \\ &+ b_1(\hat{D}_{eL}\phi_d N_3^c Y_1^4) + b_2(\hat{D}_{\mu L}\phi_d N_1^c Y_1^4) + b_3(\hat{D}_{\tau L}\phi_d N_2^c Y_1^4) \\ &+ M'_1 N_1^c N_1^c Y_1^6 + M'_2(N_2^c N_3^c Y_1^6 + N_3^c N_2^c Y_1^6), \end{aligned} \quad (18)$$

where g_i, k_i, a_i and b_i ($i = 1, 2, 3$) are coupling constants. The SUSY breaking leads to diagonal charged lepton mass matrix (Eqn. (2)) and Yukawa matrices as shown in Eqn. (4).

The vertex $\mu_{H_M} H_d \Delta_d H_d$ and $\mu_{\Delta_M} \Delta_d \phi_d \rho_d$ are invariant under the A_4 modular symmetry with μ_{H_M} and μ_{Δ_M} couplings transforming as Y_1^6 . Hence topology T4-2- i is made functioned at one-loop level. The scalar potential of the model contains supersymmetric contribution from F-terms, D-terms and soft SUSY breaking terms, defined as

$$V = V_{SUSY} + V_{soft}, \quad (19)$$

Parameter	Best fit $\pm 1\sigma$ range	3σ range
Normal neutrino mass ordering ($m_1 < m_2 < m_3$)		
$\sin^2 \theta_{12}$	$0.304^{+0.013}_{-0.012}$	$0.269 - 0.343$
$\sin^2 \theta_{13}$	$0.02221^{+0.00068}_{-0.00062}$	$0.02034 - 0.02420$
$\sin^2 \theta_{23}$	$0.570^{+0.018}_{-0.024}$	$0.407 - 0.618$
$\Delta m_{21}^2 [10^{-5} \text{eV}^2]$	$7.42^{+0.21}_{-0.20}$	$6.82 - 8.04$
$\Delta m_{31}^2 [10^{-3} \text{eV}^2]$	$+2.541^{+0.028}_{-0.027}$	$+2.431 - +2.598$
Inverted neutrino mass ordering ($m_3 < m_1 < m_2$)		
$\sin^2 \theta_{12}$	$0.304^{+0.013}_{-0.012}$	$0.269 - 0.343$
$\sin^2 \theta_{13}$	$0.02240^{+0.00062}_{-0.00062}$	$0.02053 - 0.02436$
$\sin^2 \theta_{23}$	$0.575^{+0.017}_{-0.021}$	$0.411 - 0.621$
$\Delta m_{21}^2 [10^{-5} \text{eV}^2]$	$7.42^{+0.21}_{-0.20}$	$6.82 - 8.04$
$\Delta m_{32}^2 [10^{-3} \text{eV}^2]$	$-2.497^{+0.028}_{-0.028}$	$-2.583 - -2.412$

Table 5: Neutrino oscillation data from NuFIT 5.0 used in the numerical analysis [28].

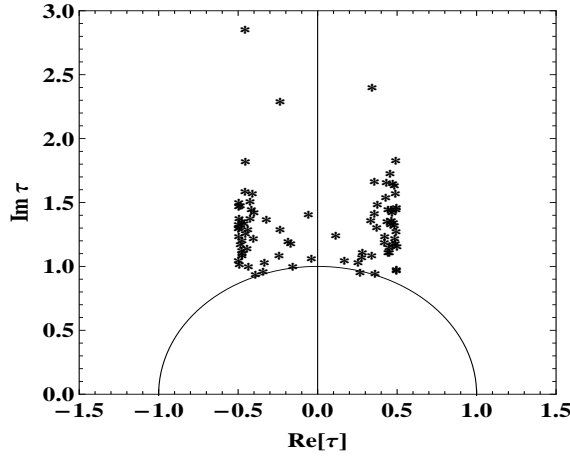


Figure 2: The parameter space of real and imaginary parts of complex modulus τ within the fundamental domain.

where F term comprises of $|F_u|^2$, $|F_d|^2$, $|F_{\Delta_u}|^2$, $|F_{\Delta_d}|^2$, $|F_{\rho_u}|^2$, $|F_{\rho_d}|^2$, $|F_{\phi_u}|^2$, $|F_{\phi_d}|^2$ and D-term contains \vec{D}^2 and D^2 which are given in Appendix B. The soft SUSY terms are given by

$$\begin{aligned}
V_{soft} = & m_{H_u}^2 |H_u|^2 + m_{H_d}^2 |H_d|^2 + m_{\Delta_d}^2 |\Delta_d|^2 + m_{\Delta_u}^2 |\Delta_u|^2 + \mu_{\rho_d} |\rho_d|^2 + \mu_{\rho_u} |\rho_u|^2 + \mu_{\phi_d} |\phi_d|^2 + \mu_{\phi_u} |\phi_u|^2 \\
& + (\mu_1^2 H_u H_d + \mu_2^2 \phi_u \phi_d + \mu_3^2 \rho_u \rho_d + \mu_4^2 \rho_u \phi_d + \mu_5^2 \phi_u \rho_d + h.c.) + \mu_{\Delta} \text{Tr}(\Delta_u \Delta_d) \\
& + (\mu_6 H_u \Delta_u H_u + \mu_7 H_d \Delta_d H_d + \mu_8 \rho_u \Delta_u \phi_u + \mu_9 \rho_d \Delta_d \phi_d + h.c.).
\end{aligned} \tag{20}$$

The soft SUSY breaking leads to the *vev* of $H_{u,d}$, $\Delta_{u,d}$ giving charged lepton masses and neutrino masses at one-loop through inert scalar fields ϕ and ρ having zero *vev*.

3 Numerical Analysis

In Eqn. (9), apart from the common scale factor the neutrino mass matrix is function of g_i , k_i ($i = 1, 2, 3$) and Yukawa couplings having modular weight 4. In general, the Yukawa couplings of higher modular weight

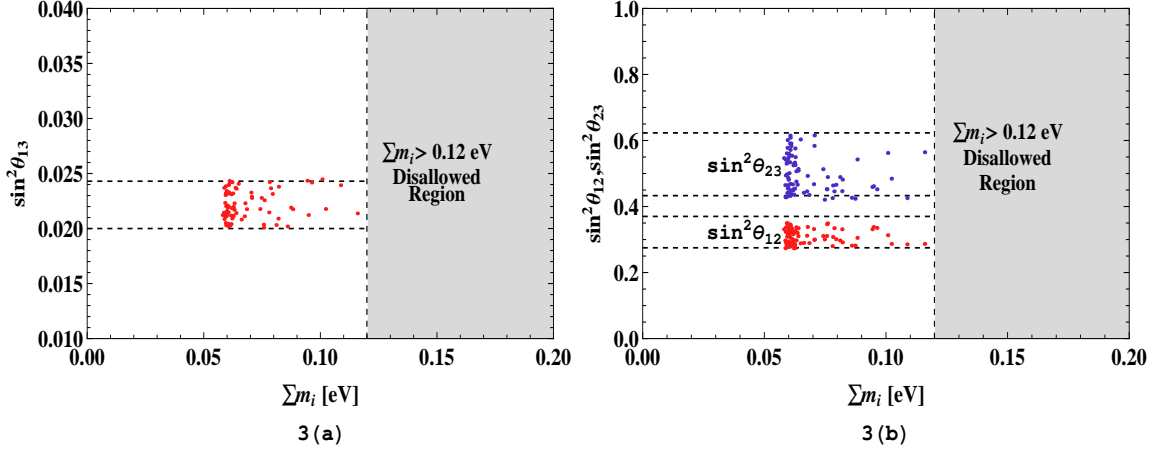


Figure 3: The variation of neutrino mixing angles with sum of neutrino masses $\sum m_i$ for Normal hierarchy. The grey shaded region is disallowed by cosmological bound on sum of neutrino masses [30,31]. The horizontal lines represent 3σ ranges of the mixing angle (Table 5).

(4, 6, 8...) are dependent on Yukawa couplings of modular weight 2 which in turn is function of complex modulus τ . In numerical analysis, the coupling constants, real and imaginary parts of τ and masses of BSM fields are varied randomly within the ranges given by

$$g_i \in [0.01, 1]; \quad k_i \in [0.01, 1]; \quad |Re(\tau)| \in [0, 0.5]; \quad Im(\tau) \in [0, 1], \\ M_k \in [1, 10^3] \text{ GeV} \quad (M_1 < M_2 < M_3); \quad M_{\rho, \phi} \in [1, 5] \text{ TeV},$$

to diagonalize \tilde{M}_ν (defined in Eqn. (9)), giving the mass eigenvalues \tilde{m}_i . The scale factor \mathcal{K} is obtained on comparison with atmospheric mass-squared difference (Δm_{31}^2), using the Eqn. (10). Using the scale factor, the neutrino mass-eigenvalues $m_i = \mathcal{K}\tilde{m}_i$ and corresponding neutrino mixing angles are evaluated using Eqn. (12). We have used experimental constraints on neutrino mixing angles ($\theta_{12}, \theta_{23}, \theta_{13}$) and solar mass-squared difference (Δm_{21}^2) to ascertain the allowed parameter space of the model. In addition, the Yukawa couplings obey the perturbative constraint $Y \leq \sqrt{4\pi}$ [29].

In the Fig. 2, we have depicted the allowed parameter space of complex modulus (τ) in the complex plane. For the allowed parameter space, imaginary part of complex modulus τ take values greater than one which serves as the source of CP violation. It is evident from Fig. 3(a) and 3(b) that the model predicts neutrino mixing angles in consonance with the 3σ experimental ranges given in Table 5. The effective Majorana neutrino mass, M_{ee} , is an important parameter which could shed the light on the nature of neutrino being Dirac or Majorana particle. In Fig. 4, we have shown ($\sum m_i - M_{ee}$) correlation plot. In fact, the model reproduces the general features of $\sum m_i - M_{ee}$ correlation plot in which M_{ee} can be vanishing near the lower bound of $\sum m_i$. Also, there is an upward shift in the lower bound on M_{ee} as $\sum m_i$ moves towards cosmological upper bound [30,31]. For example, if $\sum m_i = 0.095 \text{ eV}$ then, at 3σ , $M_{ee} > 0.012 \text{ eV}$ which is within the sensitivity reach of $0\nu\beta\beta$ decay experiments such as SuperNEMO [32], KamLAND-Zen [33], NEXT [34,35], nEXO [36]. Furthermore, the complex modulus τ is the only source of CP -violation which can be estimated in terms of CP -invariants. The Jarlskog CP invariant, J_{CP} , related to the Dirac CP -phase and I_1, I_2 related to the Majorana phases (α, β) have been defined in Eqns. (13) and (14), respectively. The predictions for these CP invariants are shown in Fig. 5. It is evident from Fig. 5(a) and 5(b) that $|J_{CP}|, |I_2| \leq 0.15$ whereas $|I_1| \leq 0.45$. In general, the model predicts existence of both CP conserving and violating solutions. Also, we have plotted the Dirac CP -violating phase (δ) with the imaginary part of complex modulus τ as shown in Fig. 6. Furthermore, we have scanned the parameter space for inverted hierarchy (IH). We find that model does not satisfy the neutrino oscillation data for IH. In particular, the reactor mixing angle ($\sin^2 \theta_{13}$) (Fig. 7(a)) and atmospheric mixing angle ($\sin^2 \theta_{23}$) (Fig. 7(b)) are found to

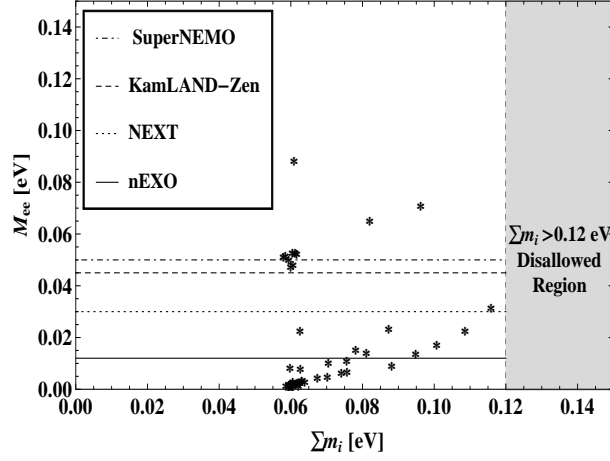


Figure 4: The variation of Effective Majorana mass M_{ee} with sum of neutrino masses $\sum m_i$ for normal hierarchical neutrino masses. The horizontal lines are the projective sensitivities of the $0\nu\beta\beta$ decay experiments. The grey shaded region is disallowed by cosmological bound on sum of the neutrino masses [30,31].

be consistent with 3σ experimental ranges while $\sin^2 \theta_{12}$ lies outside the 3σ experimental range as shown in Fig. 7(b).

4 Implications for Dark Matter (DM) and Lepton Flavor Violation (LFV)

The T4-2- i topology generates the neutrino masses at one-loop level with particles running in the loop as potential DM candidates. The scalar potential relevant for inert doublet(ρ) is

$$V_{scalar} \supset \mu_\rho^2 |\rho|^2 + \lambda_2 |\rho|^4 + \lambda_3 |H|^2 |\rho|^2 + \lambda_4 |H^\dagger \rho|^2 + \lambda_5 [(H^\dagger \rho)^2 + h.c.] + \lambda_6 (\rho^\dagger \rho) Tr[\Delta^\dagger \Delta] + \lambda_7 \rho^\dagger \Delta \Delta^\dagger \rho, \quad (21)$$

where λ_5 transforms as Y_6^1 and μ_ρ^2 , $\lambda_{2,3,4}$ includes the factor $1/(-i\tau + i\bar{\tau})^n$. After spontaneous symmetry breaking, Higgs and scalar triplet field acquire $vevs$ while inert doublet(ρ) have zero vev ,

$$\langle H \rangle = \frac{1}{\sqrt{2}} \begin{pmatrix} 0 \\ v+h \end{pmatrix}, \quad \langle \Delta \rangle = \frac{1}{\sqrt{2}} \begin{pmatrix} 0 & 0 \\ v_\Delta + T & 0 \end{pmatrix}, \quad \rho = \frac{1}{\sqrt{2}} \begin{pmatrix} \rho_1 + i\rho_2 \\ \sqrt{2}\rho^- \end{pmatrix}. \quad (22)$$

The masses of neutral(ρ_1, ρ_2) and charged components(ρ^\pm) of inert doublet are given by

$$M_{\rho_1, \rho_2}^2 = \mu_\rho^2 + \frac{\lambda_3 \pm \lambda_5}{2} v^2 + \frac{\lambda_6}{2} v_\Delta^2, \quad (23)$$

$$M_{\rho^\pm}^2 = \mu_\rho^2 + \frac{\lambda_3 + \lambda_4}{2} v^2 + \frac{\lambda_6 + \lambda_7}{2} v_\Delta^2. \quad (24)$$

Here, we have assumed the mixing between neutral components of inert doublets ρ and ϕ to be small, thus, neglected in the following analyses of DM and LFV (however, mixing is required for generating non-zero neutrino masses). For simplification, we take masses of $\rho^\pm(\phi^\pm)$, $\rho_1(\phi_1)$, $\rho_2(\phi_2)$ to be equal to $M_\rho(M_\phi)$. The relic density observed by the Planck collaboration is, [50]

$$\Omega h^2 = 0.120 \pm 0.001.$$

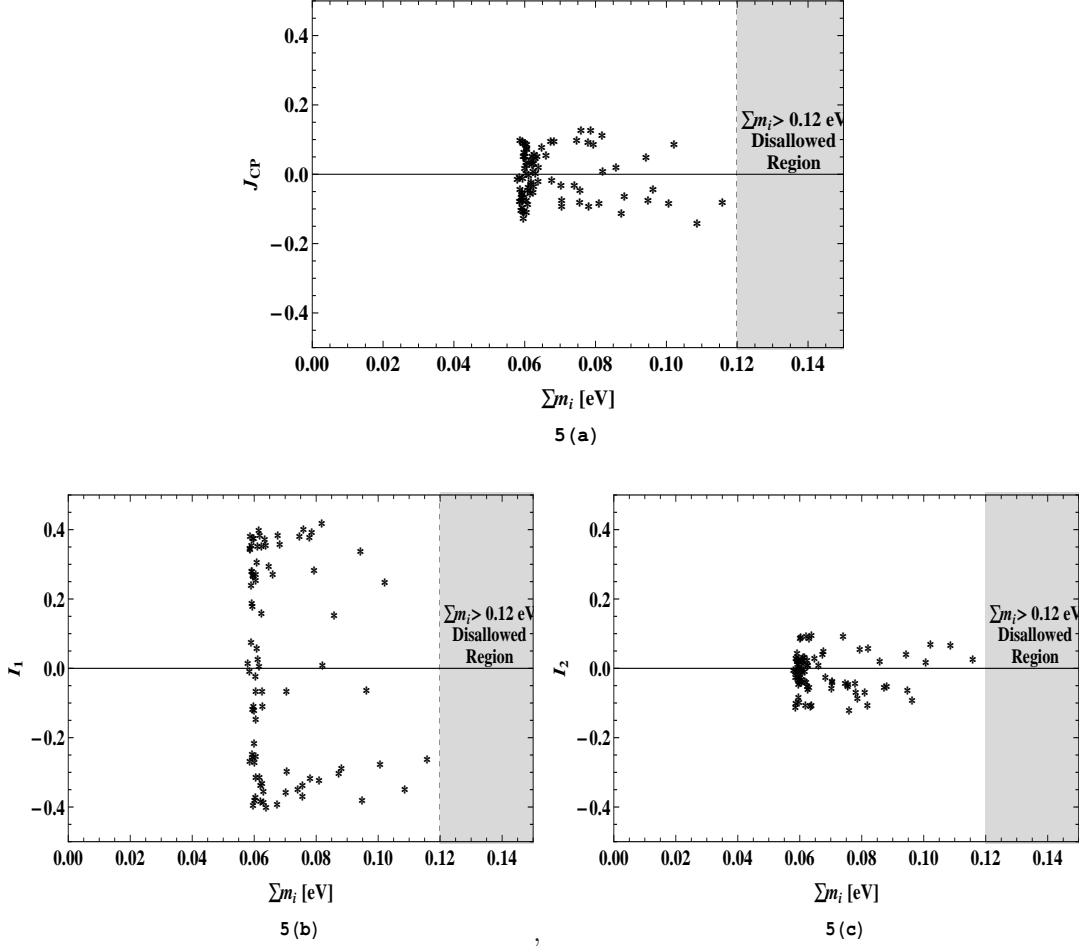


Figure 5: The variation of CP invariants J_{CP} , I_1 and I_2 with sum of neutrino masses $\sum m_i$.

We have explored the scenario of fermionic dark matter where the lightest right-handed neutrino (N_1) serves as the dark matter candidate. In case, the right-handed neutrino masses are close to each other i.e. $\Delta_i = (M_i - M_1)/M_1 \ll 1$, the co-annihilation effects are significant leading to DM relic abundance [51]

$$\Omega_{N_1} h^2 \approx \frac{3 \times 10^{-26} \text{cm}^3 \text{s}^{-1}}{\sigma_{eff}}, \quad (25)$$

where σ_{eff} is the effective cross-section containing co-annihilation effects given by [52]

$$\sigma_{eff} = \sum_{i,k=1}^3 \frac{4}{g_{eff}} (1 + \Delta_i)^{3/2} (1 + \Delta_k)^{3/2} \times e^{-x_f(\Delta_i + \Delta_k)} \langle \sigma_{ik} v_r \rangle, \quad (26)$$

x_f is freeze-out temperature and g_{eff} is the effective multiplicity at freeze-out defined as

$$g_{eff}(x_f) = \sum_{i=1}^3 2(1 + \Delta_i)^{3/2} e^{-x_f \Delta_i}. \quad (27)$$

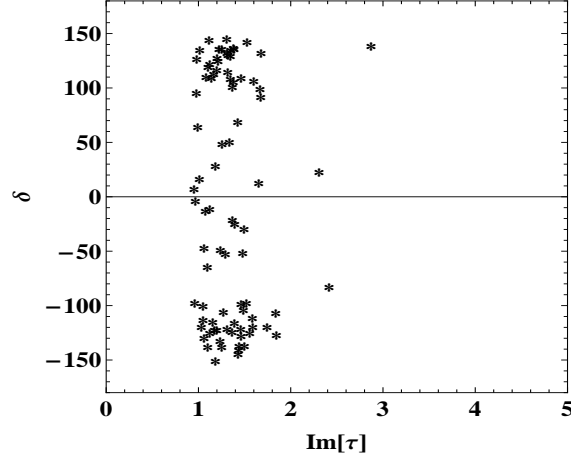


Figure 6: The variation of Dirac CP phase δ with the imaginary part of complex modulus τ .

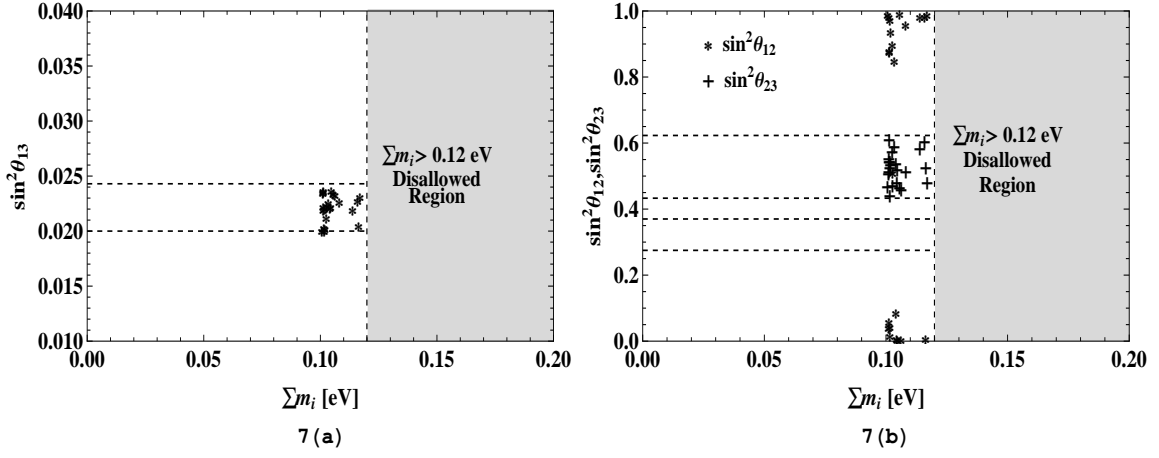


Figure 7: The variation of neutrino mixing angles with sum of neutrino masses $\sum m_i$ for inverted hierarchy. The grey shaded region is disallowed by cosmological bound on sum of neutrino masses [30,31]. The horizontal lines represent 3σ ranges of the mixing angles (Table 5).

The thermally averaged cross-section is given by [52]

$$\begin{aligned}
 v_r \sigma = & \frac{|Y_{\rho\alpha i} Y_{\rho\beta k}^*|^2}{32\pi} \frac{\sqrt{s^2 - 2s(m_{l_\alpha}^2 + m_{l_\beta}^2)^2 + (m_{l_\alpha}^2 - m_{l_\beta}^2)^2}}{s^2 - (M_i^2 - M_k^2)^2} \left[\frac{A_1 - Q - Q_2}{A_1} + \frac{Q_1 Q_2}{A_1^2} \left(1 + \frac{B^2}{A_1^2} \right) \right. \\
 & \left. + \delta_{ik} \left\{ \frac{A_2 - Q - Q_2}{A_1} + \frac{Q_1 Q_2}{A_2^2} \left(1 + \frac{B^2}{A_1^2} \right) - \frac{2M_i^2(s - m_{l_\alpha}^2 - m_{l_\beta}^2)}{A_2^2} \right\} \right], \quad (28)
 \end{aligned}$$

where $Y_{\rho\alpha i}$ is couplings of annihilation process of right-handed neutrino into charged leptons ($N_i N_k \rightarrow l_\alpha l_\beta^+$)

mediated by charged component of inert Higgs ρ , $m_{l_{\alpha,\beta}}$ are charged lepton masses and

$$\begin{aligned}
Q_1 &= M_i^2 + m_{l_\alpha}^2 - M_{\rho^+}^2 & Q_2 &= M_k^2 + m_{l_\beta}^2 - M_{\rho^+}^2, \\
A_1 &= \frac{M_i^2 + M_k^2 + m_{l_\alpha}^2 + m_{l_\beta}^2 - 2M_{\rho^+}^2 - s}{2} - \frac{(M_i^2 - M_k^2)(m_{l_\alpha}^2 - m_{l_\beta}^2)}{2s}, \\
A_2 &= M_i^2 - M_{\rho^+}^2 - \frac{(m_{l_\alpha}^2 + m_{l_\beta}^2 - s)}{2}, \\
B &= 2 \frac{\sqrt{s^2 - 2s(m_{l_\alpha}^2 + m_{l_\beta}^2) + (m_{l_\alpha}^2 - m_{l_\beta}^2)^2}}{2\sqrt{s}} p,
\end{aligned}$$

$p = \sqrt{s^2 - 2s(M_i^2 + M_k^2) + (M_i^2 - M_k^2)^2}/2\sqrt{s}$ is momentum of the incoming right-handed neutrino in the center of mass(COM) frame and s is the total energy of the system in COM frame. Also, there is no direct coupling of right-handed neutrino with Higgs boson or Z gauge boson. The effective coupling (y_{eff}) at one-loop contributes to spin independent(SI) scattering cross-section [53]

$$\sigma_{det} = \frac{y_{eff}^2 (m_N - \frac{7}{9}m_B)^2 m_N^2 M_1^2}{4\pi v^2 m_h^4 (m_N + M_1)^2}, \quad (29)$$

where m_N , m_B are nucleon and baryon masses in the chiral limit. The effective coupling y_{eff} is given by

$$\begin{aligned}
y_{eff} &= \frac{\lambda_3 v \sum_\alpha |Y_{\rho\alpha 1}|^2}{16\pi^2 M_1^3} \left(M_1^2 + (M_{\rho^+}^2 - M_1^2) \ln \left(\frac{M_{\rho^+}^2 - M_1^2}{M_{\rho^+}^2} \right) \right) \\
&\quad - \frac{(\lambda_3 + \lambda_4/2) \sum_\alpha |Y_{\rho\alpha 1}|^2}{16\pi^2 M_1^3} \left(M_1^2 + (\bar{m}^2 - M_1^2) \ln \left(\frac{\bar{m}^2 - M_1^2}{\bar{m}^2} \right) \right), \quad (30)
\end{aligned}$$

where \bar{m} is the average mass of neutral components of inert doublet ρ . Furthermore, the lepton flavor violation which is highly suppressed in SM can have significant contribution due to new fields introduced by the topology. The most stringent upper bound on LFV branching ratios comes from $\mu \rightarrow e\gamma$ decay [54,55]

$$Br(\mu \rightarrow e\gamma) < 4.2 \times 10^{-13}.$$

In the model, lepton flavor violation occurs via the mediation of charged and neutral components of inert doublets and right-handed neutrinos which is given by [56]

$$Br(\mu \rightarrow e\gamma) = \frac{3\alpha v^4}{32\pi} \left| \sum_{i=1}^3 \sum_{x=\rho,\phi} \frac{Y_{x e i}^* Y_{x \mu i}}{M_x^2} F(M_i^2/M_{x^+}^2) \right|^2, \quad (31)$$

where α is structure constant, v is vacuum expectation value of the Higgs field. The function $F(x)$ ($x = \frac{M_i^2}{M_{\rho^+}^2}$) is defined as

$$F(x) = \frac{1 - 6x + 3x^2 + 2x^3 - 6x^2 \log x}{6(1 - x^4)}.$$

In the numerical analysis, we employed the upper bound on branching ratio of lepton flavor violation process $\mu \rightarrow e\gamma$ and obtain predictions on relic density of DM and SI scattering cross-section for DM direct detection.

In Fig. 8(a), the prediction on relic density of dark matter as a function of dark matter mass ($M_{DM} = M_1$) is shown. It can be seen that model satisfies the observed relic density in the range $M_{DM} \in (1 - 10^3)$ GeV. Also, it is evident from Fig.8(b) that model predicts LFV consistent with bound coming from $\mu \rightarrow e\gamma$ process. Further, the implications of the model for dark matter direct detection are shown in Fig. 9. The points are below the experimental bound of XENON1T [57–59]. In fact, there is substantial parameter space above neutrino scattering background [60,61] which can be probed in the future DM detection experiments.

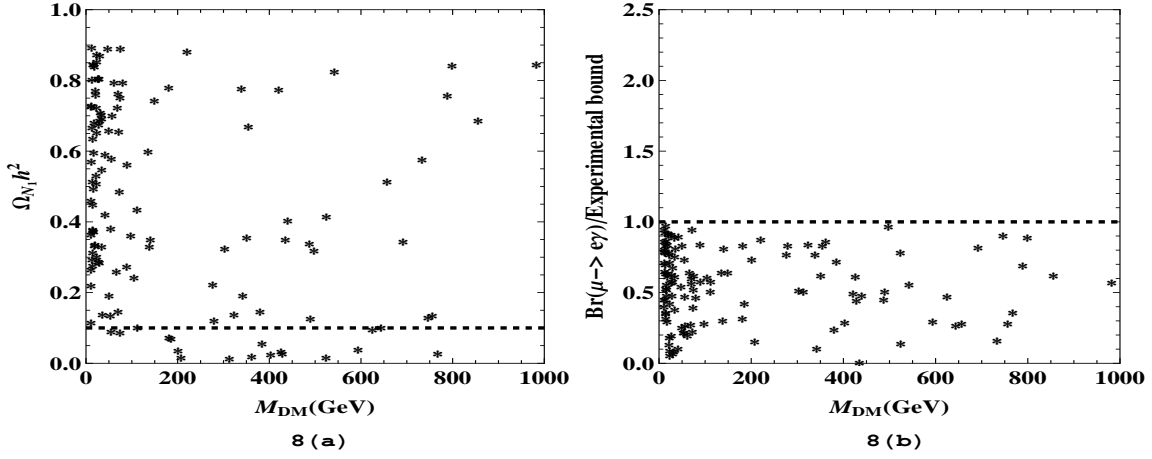


Figure 8: The relic density of dark matter and normalized branching ratio of lepton flavor violating (LFV) process $\mu \rightarrow e\gamma$ as a function of dark matter mass (M_{DM}). The horizontal lines are the observed relic density of dark matter (Fig. 8(a)) and upper bound on LFV process $Br(\mu \rightarrow e\gamma) < 4.2 \times 10^{-13}$ (Fig. 8(b)), respectively.

5 Conclusions

Out of six topologies of one-loop Weinberg operator at dimension-5, the finite Lorentz structures of T4 topology corresponds to one-loop extension of canonical seesaw scenarios. T4 topology(category (iii)) allows dominant tree-level contribution in addition to one-loop contribution to neutrino mass regardless of imposition of discrete or $U(1)$ symmetry [15]. The discrete or $U(1)$ symmetries have been employed to inhibit tree-level contribution but this requires either enlargement in the field content [24] or neutrino masses are generated by higher dimensional Weinberg operator [22]. In this work, we propose a possible alternative way to inhibit tree-level contribution wherein one may not require additional fields (fields other than required by the topology) provided we work within the paradigm of modular symmetry. Specifically, we have constructed a possible realization of T4-2- i topological Lorentz structure based on A_4 modular symmetry wherein neutrino masses are generated through one-loop dimension-5 Weinberg operator. The odd modular weight of loop particles *viz.* right-handed Majorana neutrinos (N_i), inert doublets (ρ, ϕ) ensures the dark matter stability. The model predictions for neutrino mixing angles and mass-squared differences are found to be in consonance with the current neutrino oscillation data. We have, also, obtained the implication on effective Majorana mass M_{ee} and CP invariants as shown in Figs. 4 and 5, respectively. In fact, for $\sum m_i = 0.10$ eV, the effective Majorana mass $M_{ee} > 0.012$ eV, at 3σ , which is within the sensitivity reach of $0\nu\beta\beta$ decay experiments. The model, in general, is consistent with both CP conserving and violating solutions. In this work, we have, also, explored the possibility of fermionic dark matter where one of the right-handed neutrino (N_1) is assumed to be lightest. We have obtained the predictions of the model for relic density of DM and its implication for direct searches experiments while obeying the bound from lepton number violating process $\mu \rightarrow e\gamma$. We find that the model explains observed relic density for the DM mass in the range $(1 - 10^3)$ GeV. Furthermore, SI scattering cross-section is found to be below the experimental bound of XENON1T and substantial parameter space above neutrino scattering background is viable which can be probed in the future DM direct detection experiments.

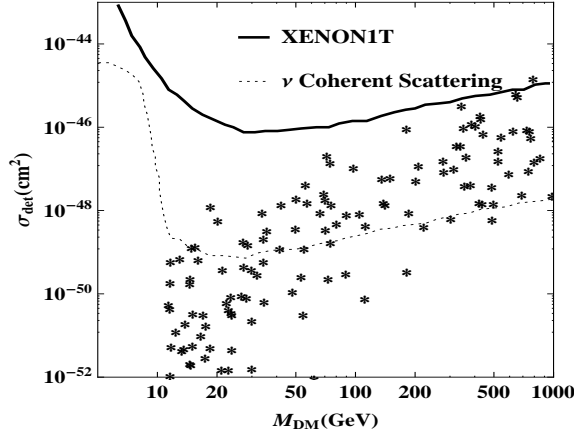


Figure 9: The SI scattering cross-section for direct detection of DM as a function of dark matter mass(M_{DM}) with the exclusion bound from XENON1T experiment. The dashed line represents the bound of irreducible neutrino background.

Appendix A Modular symmetry and Permutation groups

For a complex number τ , the linear fractional transformations are defined as

$$\gamma : \tau \rightarrow \gamma(\tau) = \frac{a\tau + b}{c\tau + d}, \quad (32)$$

where a, b, c and d are integers(Z) obeying the condition $ad - bc = 1$. These linear fractional transformations acting on the upper-half of the complex plane constitute modular group (Γ). The generators of the modular group satisfy the relations $S^2 = I$ and $(ST)^3 = I$ and are defined by matrices

$$S = \begin{pmatrix} 0 & 1 \\ -1 & 0 \end{pmatrix}; \quad T = \begin{pmatrix} 1 & 1 \\ 0 & 1 \end{pmatrix}.$$

The action of these generators on the complex plane is defined as

$$S : \tau \rightarrow -\frac{1}{\tau}, \quad T : \tau \rightarrow \tau + 1.$$

Also, $\Gamma(N)$ is defined as series of groups given by

$$\Gamma(N) = \left\{ \begin{bmatrix} a & b \\ c & d \end{bmatrix} \in SL(2, Z), \begin{bmatrix} a & b \\ c & d \end{bmatrix} = \begin{bmatrix} 1 & 0 \\ 0 & 1 \end{bmatrix} \pmod{N} \right\}, \quad (33)$$

where, $SL(2, Z)$ is a special linear group of 2×2 matrices with unit determinant and $\Gamma(1) = SL(2, Z)$. In general, γ and $-\gamma$ result in identical linear transformations however, distinct linear transformations form series of infinite modular groups $\bar{\Gamma}(N)$ such that $\bar{\Gamma} = \bar{\Gamma}(1) = \Gamma(1)/\{I, -I\} = PSL(2, Z)$. The quotient group of infinite modular groups defined as $\Gamma_N = \bar{\Gamma}/\bar{\Gamma}(N)$ leads to finite Modular groups. These groups (Γ_N) are isomorphic to the permutation groups such as $\Gamma_2 \simeq S_3$ [37, 38], $\Gamma_3 \simeq A_4$ [39–43], $\Gamma_4 \simeq S_4$ [44–46] and $\Gamma_5 \simeq A_5$ [47, 48].

In general, fractional linear transformations are very constraining and are not trivial to be exactly preserved, however, one may define the modular forms, $f(\tau)$ as holomorphic functions of complex modulus τ such that fractional linear transformations preserve the zeroes and poles of $f(\tau)$. Under the transformation properties of $\Gamma(N)$, described in Eqns. (32) and (33), level N modular forms are defined as

$$f(\gamma\tau) = (c\tau + d)^{2k} f(\tau), \quad (34)$$

where

$$\gamma = \begin{bmatrix} a & b \\ c & d \end{bmatrix} \in \Gamma(N),$$

up to the factor $(c\tau + d)^{2k}$ with modular weight $2k$. In general, modular forms are invariant under $\Gamma(N)$, however, they do transform under finite modular group Γ_N . In fact, It result in a unique feature of the finite modular groups that Yukawa couplings transform under the modular symmetry. In unitary representation, the modular transformations can be written as

$$f(\tau) \rightarrow e^{i\alpha} (c\tau + d)^k f(\tau). \quad (35)$$

In particular, for modular weight 2, Eqn. (35) result in

$$\frac{d}{d\tau} \log f(\tau) \rightarrow (c\tau + d)^2 \frac{d}{d\tau} \log f(\tau) + kc(c\tau + d),$$

such that the last term $kc(c\tau + d)$ should vanish. Similarly, it should, also, vanish for all higher modular weights to preserve the fractional linear transformations. This leads to the constraint $\sum k_i = 0$ if Γ_N modular symmetry is to be preserved. The Dedekind η -function and its derivative can be used to construct modular forms of weight 2 as [49]

$$\begin{aligned} Y_1^2(\tau) &= \frac{i}{2\pi} \left[\frac{\eta'(\tau/3)}{\eta(\tau/3)} + \frac{\eta'((\tau+1)/3)}{\eta((\tau+1)/3)} + \frac{\eta'((\tau+2)/3)}{\eta((\tau+2)/3)} - 27 \frac{\eta'(3\tau)}{\eta(3\tau)} \right], \\ Y_2^2(\tau) &= \frac{-i}{\pi} \left[\frac{\eta'(\tau/3)}{\eta(\tau/3)} + \omega^2 \frac{\eta'((\tau+1)/3)}{\eta((\tau+1)/3)} + \omega \frac{\eta'((\tau+2)/3)}{\eta((\tau+2)/3)} \right], \\ Y_3^2(\tau) &= \frac{-i}{\pi} \left[\frac{\eta'(\tau/3)}{\eta(\tau/3)} + \omega \frac{\eta'((\tau+1)/3)}{\eta((\tau+1)/3)} + \omega^2 \frac{\eta'((\tau+2)/3)}{\eta((\tau+2)/3)} \right], \end{aligned} \quad (36)$$

where $\omega = e^{i2\pi/3}$ and $Y_2^2 + 2Y_1^2Y_3^2 = 0$.

These modular forms of weight 2 can be arranged as A_4 triplet *viz.*

$$Y = \begin{pmatrix} Y_1^2 \\ Y_2^2 \\ Y_3^2 \end{pmatrix}.$$

Also, modular forms of higher weights (2, 4, 6, 8, ...) can be constructed using modular forms of weight 2. For example, the Yukawa couplings of modular weight 4 consists of two singlets 1, 1' and one triplet 3 as

$$Y_1^4 = ((Y_1^2)^2 + 2Y_2^2Y_3^2), \quad Y_{1'}^4 = ((Y_3^2)^2 + 2Y_1^2Y_2^2), \quad Y_3^4 = \begin{pmatrix} (Y_1^2)^2 - Y_2^2Y_3^2 \\ (Y_3^2)^2 - Y_1^2Y_2^2 \\ (Y_2^2)^2 - Y_1^2Y_3^2 \end{pmatrix}.$$

It is to be noted that, in numerical analysis, we have used the q -expansion of modular forms using Dedekind η -function defined in upper-half of the complex plane as

$$\eta(\tau) = q^{1/24} \sum_{n=1}^{\infty} (1 - q^n), \quad (37)$$

where $q = e^{i2\pi\tau}$. For the Yukawa couplings of modular weight 2, the q -expansions of Dedekind eta-function is

$$\begin{aligned} Y_1^2(\tau) &= 1 + 12q + 36q^2 + 12q^3 + \dots, \\ Y_2^2(\tau) &= -6q^{1/3} (1 + 7q + 8q^2 + \dots), \\ Y_3^2(\tau) &= -18q^{2/3} (1 + 2q + 5q^2 + \dots). \end{aligned} \quad (38)$$

Appendix B Supersymmetric Scalar Potential

The F-terms are given by

$$\begin{aligned}
|F_u|^2 &= |\mu_1^2 H_d + \lambda_3 \Delta_u H_u|, \\
|F_d|^2 &= |\mu_1^2 H_u + \lambda_u \Delta_d H_d|, \\
|F_{\Delta_u}|^2 &= |\mu \Delta_d + \lambda_3 H_u H_d + \lambda_6 \rho_D \phi u|, \\
|F_{\Delta_d}|^2 &= |\mu \Delta_u + \lambda_4 H_d H_d + \lambda_5 \rho_u \phi_d|, \\
|F_{\rho_\mu}|^2 &= |\mu_3^2 \rho_d + \mu_4^2 \Phi_u + \lambda_5 \Delta_d \Phi_d|, \\
|F_{\rho_d}|^2 &= |\mu_3^2 \rho_u + \mu_5^2 \Phi_d + \lambda_6 \Delta_u \Phi_u|, \\
|F_{\Phi_\mu}|^2 &= |\mu_2^2 \Phi_d + \mu_4^2 \rho_u + \lambda_6 \rho_d \Delta_u|, \\
|F_{\Phi_d}|^2 &= |\mu_2^2 \Phi_u + \mu_5^2 \rho_d + \lambda_5 \rho_u \Delta_d|,
\end{aligned}$$

while D-terms are

$$D^2 = \frac{g_1^2}{2} \left[\frac{1}{2} \left(H_u^\dagger H_u - H_d^\dagger H_d + \text{Tr}(\Delta_d^\dagger \Delta_d) - \text{Tr}(\Delta_u^\dagger \Delta_u) \right) \right]^2,$$

and

$$\vec{D}^2 = \frac{g_2^2}{2} \sum_{a=1}^3 \left[\frac{1}{2} \left(H_u^\dagger \sigma^a H_u + H_d^\dagger \sigma^a H_d + \frac{1}{2} \text{Tr}(\Delta_d^\dagger [\sigma^a, \Delta_d]) + \frac{1}{2} \text{Tr}(\Delta_u^\dagger [\sigma^a, \Delta_u]) \right) \right]^2.$$

Acknowledgments

M. K. acknowledges the financial support provided by Department of Science and Technology(DST), Government of India vide Grant No. DST/INSPIRE Fellowship/2018/IF180327. The authors, also, acknowledge Department of Physics and Astronomical Science for providing necessary facility to carry out this work.

References

- [1] S. Weinberg, *Baryon and Lepton Nonconserving Processes*, *Phys. Rev. Lett.* **43** (1979) 1566-1570.
- [2] P. Minkowski, $\mu \rightarrow e\gamma$ at a Rate of One Out of 10^9 Muon Decays?, *Phys. Lett. B* **67** (1977) 421-428.
- [3] R. N. Mohapatra and G. Senjanovic, *Neutrino Mass and Spontaneous Parity Nonconservation*, *Phys. Rev. Lett.* **44** (1980) 912.
- [4] M. Magg and C. Wetterich, *Neutrino Mass Problem and Gauge Hierarchy*, *Phys. Lett. B* **94** (1980) 61-64.
- [5] J. Schechter and J. W. F. Valle, *Neutrino Masses in $SU(2) \times U(1)$ Theories*, *Phys. Rev. D* **22** (1980) 2227.
- [6] C. Wetterich, *Neutrino Masses and the Scale of B-L Violation*, *Nucl. Phys. B* **187** (1981) 343-375.
- [7] R. Foot, H. Lew, X. G. He and G. C. Joshi, *Seesaw Neutrino Masses Induced by a Triplet of Leptons*, *Z. Phys. C* **44** (1989) 441.
- [8] R. N. Mohapatra and J. W. F. Valle, *Neutrino Mass and Baryon Number Nonconservation in Superstring Models*, *Phys. Rev. D* **34** (1986) 1642.
- [9] E. K. Akhmedov, M. Lindner, E. Schnapka and J. W. F. Valle, *Left-right symmetry breaking in NJL approach*, *Phys. Lett. B* **368** (1996) 270-280.

- [10] E. K. Akhmedov, M. Lindner, E. Schnapka and J. W. F. Valle, *Dynamical left-right symmetry breaking*, *Phys. Rev. D* **53** (1996) 2752-2780.
- [11] Y. Cai, J. Herrero-García, M. A. Schmidt, A. Vicente and R. R. Volkas, *From the trees to the forest: a review of radiative neutrino mass models*, *Front. in Phys.* **5** (2017) 63.
- [12] C. S. Aulakh and R. N. Mohapatra, *Neutrino as the Supersymmetric Partner of the Majoron*, *Phys. Lett. B* **119** (1982) 136-140.
- [13] J. R. Ellis, G. Gelmini, C. Jarlskog, G. G. Ross and J. W. F. Valle, *Phenomenology of Supersymmetry with Broken R-Parity*, *Phys. Lett. B* **150** (1985) 142-148.
- [14] A. Abada, S. Davidson and M. Losada, *Neutrino masses and mixings in the MSSM with soft bilinear $R(p)$ violation*, *Phys. Rev. D* **65** (2002) 075010.
- [15] F. Bonnet, M. Hirsch, T. Ota and W. Winter, *Systematic study of the $d=5$ Weinberg operator at one-loop order*, *JHEP* **07** (2012) 153.
- [16] D. Aristizabal Sierra, A. Degee, L. Dorame and M. Hirsch, *Systematic classification of two-loop realizations of the Weinberg operator*, *JHEP* **03** (2015) 040.
- [17] E. Ma, *Verifiable radiative seesaw mechanism of neutrino mass and dark matter*, *Phys. Rev. D* **73** (2006) 077301.
- [18] J. Kubo, E. Ma and D. Suematsu, *Cold Dark Matter, Radiative Neutrino Mass, $\mu \rightarrow e\gamma$, and Neutrinoless Double Beta Decay*, *Phys. Lett. B* **642** (2006) 18-23.
- [19] E. Ma, *$SU(5)$ completion of the dark scalar doublet model of radiative neutrino mass*, *Phys. Lett. B* **659** (2008) 885-887.
- [20] A. Zee, *A Theory of Lepton Number Violation, Neutrino Majorana Mass, and Oscillation*, *Phys. Lett. B* **93** (1980) 389. [erratum: *Phys. Lett. B* **95** (1980) 461.]
- [21] E. Ma, *Pathways to naturally small neutrino masses*, *Phys. Rev. Lett.* **81** (1998) 1171-1174.
- [22] S. Kanemura and H. Sugiyama, *Dark matter and a suppression mechanism for neutrino masses in the Higgs triplet model*, *Phys. Rev. D* **86** (2012) 073006.
- [23] W. Wang and Z. L. Han, *Radiative linear seesaw model, dark matter, and $U(1)_{B-L}$* , *Phys. Rev. D* **92** (2015) 095001.
- [24] M. A. Loualidi and M. Miskaoui, *One-loop Type II Seesaw Neutrino Model with Stable Dark Matter Candidates*, *Nucl. Phys. B* **961** (2020) 115219.
- [25] C. Jarlskog, *Commutator of the Quark Mass Matrices in the Standard Electroweak Model and a Measure of Maximal CP Nonconservation*, *Phys. Rev. Lett.* **55** (1985) 1039.
- [26] P. I. Krastev and S. T. Petcov, *Resonance Amplification and t Violation Effects in Three Neutrino Oscillations in the Earth*, *Phys. Lett. B* **205** (1988) 84-92.
- [27] J. Wess and J. Bagger, Princeton University Press, 1992, ISBN 978-0-691-02530-8.
- [28] I. Esteban, M. C. Gonzalez-Garcia, M. Maltoni, T. Schwetz and A. Zhou, *The fate of hints: updated global analysis of three-flavor neutrino oscillations*, *JHEP* **09** (2020) 178.
- [29] T. Nomura, H. Okada and O. Popov, *A modular A_4 symmetric scotogenic model*, *Phys. Lett. B* **803** (2020) 135294.
- [30] E. Giusarma, M. Gerbino, O. Mena, S. Vagnozzi, S. Ho and K. Freese, *Improvement of cosmological neutrino mass bounds*, *Phys. Rev. D* **94** (2016) 083522.

- [31] N. Aghanim *et al.* [Planck], *Planck 2018 results. VI. Cosmological parameters*, *Astron. Astrophys.* **641** (2020) A6.
- [32] A. S. Barabash, *SeperNEMO double beta decay experiment*, *J. Phys. Conf. Ser.* **375** (2012) 042012.
- [33] A. Gando *et al.* [KamLAND-Zen], *Search for Majorana Neutrinos near the Inverted Mass Hierarchy Region with KamLAND-Zen*, *Phys. Rev. Lett.* **117** (2016) 082503.
- [34] F. Granena *et al.* [NEXT], *NEXT, a HPGXe TPC for neutrinoless double beta decay searches*, arXiv:0907.4054 [hep-ex].
- [35] J. J. Gomez-Cadenas *et al.* [NEXT], *Present status and future perspectives of the NEXT experiment*, *Adv. High Energy Phys.* **2014** (2014) 907067.
- [36] C. Licciardi [nEXO], *The Sensitivity of the nEXO Experiment to Majorana Neutrinos*, *J. Phys. Conf. Ser.* **888** (2017) 012237.
- [37] T. Kobayashi, K. Tanaka and T. H. Tatsuishi, *Neutrino mixing from finite modular groups*, *Phys. Rev. D* **98** (2018) 016004.
- [38] H. Okada and Y. Orikasa, *Modular S_3 symmetric radiative seesaw model*, *Phys. Rev. D* **100** (2019) 115037.
- [39] T. Nomura and H. Okada, *A modular A_4 symmetric model of dark matter and neutrino*, *Phys. Lett. B* **797** (2019) 134799.
- [40] D. Zhang, *A modular A_4 symmetry realization of two-zero textures of the Majorana neutrino mass matrix*, *Nucl. Phys. B* **952** (2020) 114935.
- [41] H. Okada and Y. h. Qi, *Zee-Babu model in modular A_4 symmetry*, [arXiv:2109.13779 [hep-ph]].
- [42] M. K. Behera, S. Mishra, S. Singirala and R. Mohanta, *Implications of A_4 modular symmetry on neutrino mass, mixing and leptogenesis with linear seesaw*, *Phys. Dark Univ.* **36** (2022) 101027.
- [43] M. K. Behera and R. Mohanta, *Linear Seesaw in A_5' Modular Symmetry With Leptogenesis*, *Front. in Phys.* **10** (2022) 854595.
- [44] J. T. Penedo and S. T. Petcov, *Lepton Masses and Mixing from Modular S_4 Symmetry*, *Nucl. Phys. B* **939** (2019) 292-307.
- [45] S. F. King and Y. L. Zhou, *Trimaximal TM_1 mixing with two modular S_4 groups*, *Phys. Rev. D* **101** (2020) 015001.
- [46] T. Kobayashi, Y. Shimizu, K. Takagi, M. Tanimoto and T. H. Tatsuishi, *New A_4 lepton flavor model from S_4 modular symmetry*, *JHEP* **02** (2020) 097.
- [47] P. P. Novichkov, J. T. Penedo, S. T. Petcov and A. V. Titov, *Modular A_5 symmetry for flavour model building*, *JHEP* **04** (2019) 174.
- [48] G. J. Ding, S. F. King and X. G. Liu, *Neutrino mass and mixing with A_5 modular symmetry*, *Phys. Rev. D* **100** (2019) 115005.
- [49] F. Feruglio, *Are neutrino masses modular forms?*, arXiv:1706.08749 [hep-ph].
- [50] N. Aghanim *et al.* [Planck], *Planck 2018 results. VI. Cosmological parameters*, *Astron. Astrophys.* **641** (2020), A6 [erratum: *Astron. Astrophys.* **652** (2021), C4].
- [51] G. Jungman, M. Kamionkowski and K. Griest, *Supersymmetric dark matter*, *Phys. Rept.* **267** (1996), 195-373.
- [52] A. Ahriche, A. Jueid and S. Nasri, *Radiative neutrino mass and Majorana dark matter within an inert Higgs doublet model*, *Phys. Rev. D* **97** (2018) no.9, 095012.

- [53] N. Okada and T. Yamada, *Simple fermionic dark matter models and Higgs boson couplings*, *JHEP* **10** (2013), 017.
- [54] J. Adam *et al.* [MEG], *New constraint on the existence of the $\mu^+ \rightarrow e^+\gamma$ decay*, *Phys. Rev. Lett.* **110** (2013) 201801.
- [55] A. M. Baldini *et al.* [MEG], *Search for the lepton flavour violating decay $\mu^+ \rightarrow e^+\gamma$ with the full dataset of the MEG experiment*, *Eur. Phys. J. C* **76** (2016) no.8 434.
- [56] A. Ahriche, *A Scotogenic Model with Two Inert Doublets*, [arXiv:2208.00500 [hep-ph]].
- [57] E. Aprile *et al.* [XENON], *Dark Matter Search Results from a One Ton-Year Exposure of XENON1T*, *Phys. Rev. Lett.* **121** (2018) no.11 111302.
- [58] E. Aprile *et al.* [XENON], *Search for Light Dark Matter Interactions Enhanced by the Migdal Effect or Bremsstrahlung in XENON1T*, *Phys. Rev. Lett.* **123** (2019) no.24 241803.
- [59] E. Aprile *et al.* [XENON], *Search for Coherent Elastic Scattering of Solar ^8B Neutrinos in the XENON1T Dark Matter Experiment*, *Phys. Rev. Lett.* **126** (2021) 091301.
- [60] J. Billard, L. Strigari and E. Figueroa-Feliciano, *Implication of neutrino backgrounds on the reach of next generation dark matter direct detection experiments*, *Phys. Rev. D* **89** (2014) no.2 023524.
- [61] J. B. Dent, B. Dutta, J. L. Newstead and L. E. Strigari, *Effective field theory treatment of the neutrino background in direct dark matter detection experiments*, *Phys. Rev. D* **93** (2016) no.7 075018.